Supporting Information

Two Solvent-Dependent Manganese(II) Supramolecular Isomers: solid-state transformation and magnetic properties

Wen-Wen Dong[a], *Dong-Sheng Li*[*,a,c], Jun Zhao[a], Lu-Fang Ma[b,*], Ya-Pan Wu[a], Ya-Ping Duan[a]

[a] *College of Mechanical & Material Engineering, Research Institute of Materials, China Three Gorges University, Yichang 443002, P. R. China*

[b] *College of Chemistry and Chemical Engineering, Luoyang Normal University, Luoyang 471022, P. R. China*

[c] *State Key Laboratory of Coordination Chemistry, Nanjing University, Nanjing 210093, P. R. China*

CrystEngComm

* Corresponding authors

E-mail: lidongsheng1@126.com. Tel./Fax: +86-717-6397516 (D.-S. Li).

mazhuxp@126.com. Tel./Fax: +86-0379-65526089(L.-F. Ma)

1. Experimental

Materials and General Methods

All solvents and reagents for syntheses were commercially available and used as received. The infrared spectra (400-4000 cm^{-1}) were recorded as KBr pellets a FTIR Nexus spectrophotometer. Elemental analyses were performed on a Perkin-Elmer 2400 Series II analyzer. Temperature-variable X-ray powder diffraction (XRPD) patterns for microcrystalline samples were taken on a Rigaku Ultima IV diffractometer (Cu Kα radiation, λ = 1.5406 Å), with a scan speed of 8 °/min and a step size of 0.02 deg in 2θ. The calculated XRPD patterns were simulated by using the single-crystal X-ray diffraction data. Thermogravimetric (TG) curves were recorded on a NETZSCH STA 449C microanalyzer in air atmosphere at a heating rate of 10ºC·min^{-1}. Variable-temperature magnetic susceptibility measurements (2-300 K) were carried out on a Quantum Design PPMS60000 in a magnetic field of 1KOe, and the diamagnetic corrections were evaluated by using Pascal's constants.

Synthesis of $[Mn_2(pbt)_2(H_2O)_2\cdot 2H_2O]_n$ (1)

A mixture of H_2pbt (0.0213g, 0.1mmol), $MnSO_4\cdot H_2O$ (0.0169g, 0.1mmol), and H_2O (8mL) was placed in a Parr Teflon-lined stainless steel (25 mL) autoclave, heated to 160°C for 3 days, and then naturally cooled to room temperature. Pale yellow crystals were obtained in a yield of 82% (based on Mn^{II}). Element analysis (%) for $C_{18}H_{18}Mn_2N_{14}O_4$ (**1**): Cald, C 35.37, H 3.00, N 32.45; Found, C 35.91, H 3.25, N 33.57. IR (cm^{-1}): 3033w, 1606s, 1567w, 1457s, 1436s, 1305s, 1275m, 1191m, 1149m, 1109m, 1017m, 999s, 796m, 749m, 723s, 683s, 675m.

Synthesis of $[Mn_2(pbt)_2(H_2O)_2\cdot DMF]_n$ (2)

A similar procedure to that of **1** except that H_2O (8 mL) was replaced by DMF-H_2O (8 mL v/v 1:1). Colorless crystals of **2** were obtained in 59% yield (based on Mn^{II}). Element analysis (%) for $C_{21}H_{21}Mn_2N_{15}O_3$ (2): Calcd, C 39.33, H 3.30, N 32.76; Found, C 39.91, H 3.27, N 33.17. IR (cm−1): 3250w, 1653s, 1505s, 1455m, 1434s, 1388w, 1363w, 1296s, 1114s, 1017m, 998m, 800s, 756s, 725s, 674m, 654s.

2. Crystallographic data collection and refinement

Single crystal X-ray diffraction analyses of compounds **1** and **2** were carried out on a Rigaku XtaLAB mini diffractometer with graphite monochromated Mo *K*α radiation (λ = 0.71073 Å). The collected data we re reduced using the program CrystalClear[1] and an empirical absorption correction was applied. The structu

re was solved by direct methods and refined based on F^2 by the full matrix least-squares methods using SHELXTL.[2] All non-H atoms were refined anisotropically. The position of hydrogen atoms attached to carbon atoms were generated geometrically (C−H bond fixed at 0.97 Å). The hydrogen atoms of water for 1 could not be reliably located but are included in the formula. The ADP values of some of pyridyl atoms and of atoms in the dimethylformamide molecule are indeed slightly larger than those of neighboring atoms, we were unable to constrain reasonable disordered models to decrease to the rational ADPs value despite many attempts to do so, assuming that was the case.

References

[1] Rigaku (2011). CrystalClear. Rigaku Americas, The Woodlands, Texas, USA, and Rigaku Corporation, Tokyo, Japan.

[2] G. M. Sheldrick, Acta Crystallogr. 2008, A64, 112.

Table S1. Selected bond lengths (Å) and bond angles(°) for **1** and **2**

1[a]			
Mn(1)-N(10)#1	2.209(3)	Mn(2)-N(3)#2	2.174(3)
Mn(1)-O(1)	2.222(3)	Mn(2)-O(2)	2.213(3)
Mn(1)-N(4)	2.268(2)	Mn(2)-N(11)	2.229(3)
Mn(1)-N(12)	2.274(3)	Mn(2)-N(1)#3	2.238(3)
Mn(1)-N(9)	2.308(3)	Mn(2)-N(5)#3	2.267(3)
Mn(1)-N(7)	2.341(3)	Mn(2)-N(14)	2.331(3)
N(10)#1-Mn(1)-O(1)	87.96(12)	N(3)#2-Mn(2)-O(2)	91.44(11)
N(10)#1-Mn(1)-N(4)	90.85(11)	N(3)#2-Mn(2)-N(11)	97.92(10)
O(1)-Mn(1)-N(4)	88.84(9)	O(2)-Mn(2)-N(11)	96.41(10)
N(10)#1-Mn(1)-N(12)	150.37(12)	N(3)#2-Mn(2)-N(1)#3	168.70(9)
O(1)-Mn(1)-N(12)	82.56(10)	O(2)-Mn(2)-N(1)#3	90.32(12)
N(4)-Mn(1)-N(12)	116.82(10)	N(11)-Mn(2)-N(1)#3	92.97(10)
N(10)#1-Mn(1)-N(9)	85.12(10)	N(3)#2-Mn(2)-N(5)#3	94.42(10)
O(1)-Mn(1)-N(9)	113.61(10)	O(2)-Mn(2)-N(5)#3	92.39(12)
N(4)-Mn(1)-N(9)	156.97(10)	N(11)-Mn(2)-N(5)#3	164.63(11)
N(12)-Mn(1)-N(9)	73.31(10)	N(1)#3-Mn(2)-N(5)#3	74.36(10)
N(10)#1-Mn(1)-N(7)	109.35(12)	N(3)#2-Mn(2)-N(14)	92.66(10)
O(1)-Mn(1)-N(7)	154.89(11)	O(2)-Mn(2)-N(14)	169.93(10)
N(4)-Mn(1)-N(7)	73.33(9)	N(11)-Mn(2)-N(14)	73.92(10)
N(12)-Mn(1)-N(7)	89.78(11)	N(1)#3-Mn(2)-N(14)	87.45(11)

N(9)-Mn(1)-N(7)	86.62(10)	N(5)#3-Mn(2)-N(14)	96.45(12)
2[b]			
Mn(1)-O(1)	2.176(3)	Mn(1)-N(2)#2	2.245(3)
Mn(1)-N(4)	2.210(3)	Mn(1)-N(6)#2	2.298(3)
Mn(1)-N(3)#1	2.216(3)	Mn(1)-N(7)	2.322(4)
O(1)-Mn(1)-N(4)	97.12(11)	O(1)-Mn(1)-N(3)#1	91.07(14)
N(6)#2-Mn(1)-N(7)	84.93(13)	N(2)#2-Mn(1)-N(7)	91.57(12)
N(3)#1-Mn(1)-N(7)	92.82(13)	N(4)-Mn(1)-N(7)	74.23(11)
O(1)-Mn(1)-N(7)	170.55(13)	N(2)#2-Mn(1)-N(6)#2	74.09(10)
N(3)#1-Mn(1)-N(6)#2	170.89(11)	N(4)-Mn(1)-N(6)#2	97.12(11)
O(1)-Mn(1)-N(6)#2	92.52(14)	N(3)#1-Mn(1)-N(2)#2	97.18(11)
N(4)-Mn(1)-N(2)#2	164.10(11)	O(1)-Mn(1)-N(2)#2	96.49(12)
N(4)-Mn(1)-N(3)#1	90.74(11)		

[a] Symmetry codes for **1**: #1 -x+1, y, -z+1/2; #2 -x+1, -y, -z; #3 x-1/2, -y+1/2, -z;

[b] Symmetry codes for **2:** #1 y-5/4, -x+5/4, -z+1/4; # 2 -y+5/4, x+3/4, z-1/4.

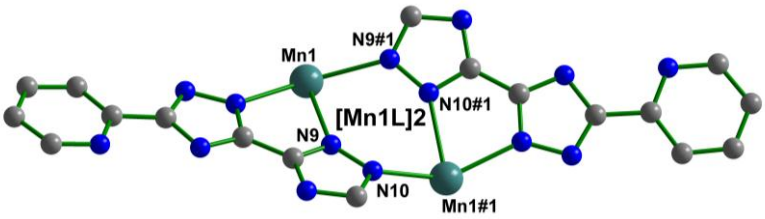

Figure S1. Ball-and-stick representation of $[Mn1(trz)]_2$ dimeric unit in **1**.

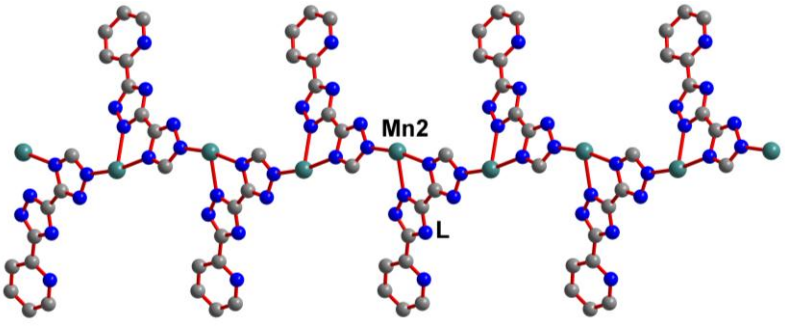

Figure S2. Ball-and-stick representation of [Mn2(pbt)] polymeric zigzag chains in **1**.

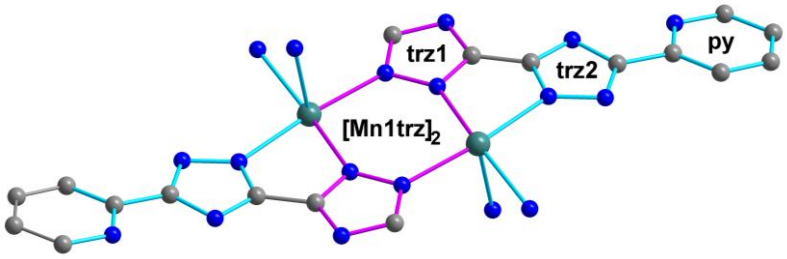

Figure S3. Ball-and-stick representation of $[Mn1(trz)]_2$ dimeric unit in **2**.

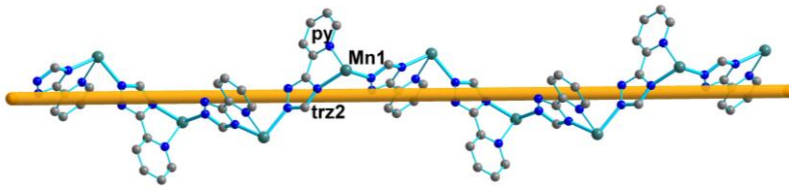

Figure S4. Ball-and-stick representation of [Mn1(pbt)] 4_1 helical chains in **2**.

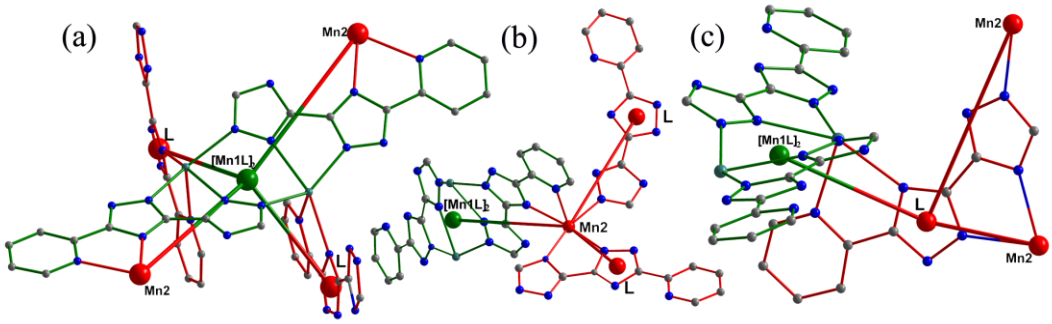

Figure S5. Ball-and-stick representation of four-connected dimeric Mn^{II}-unit, three-connected $Mn2^{II}$ ion and pbt^{2-} ligand in compound **1**.

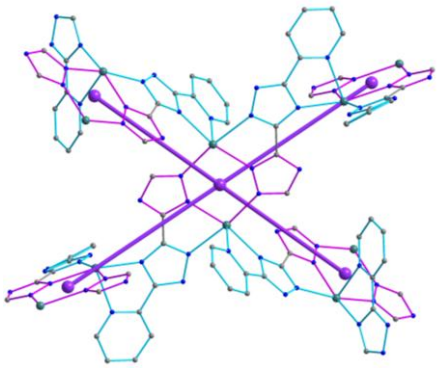

Figure S6. Ball-and-stick representation of four-connected dimeric Mn^{II}-unit in compound **2**.

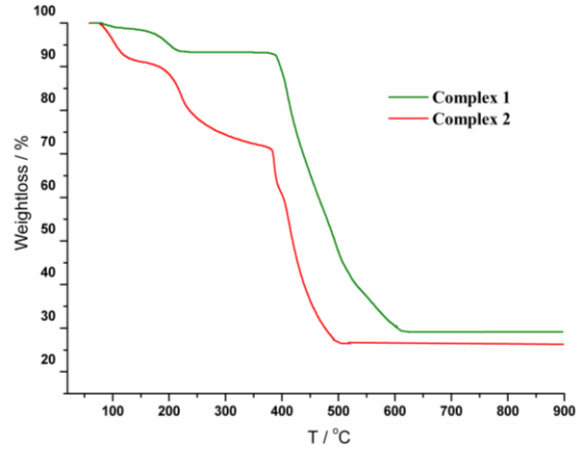

Figure S7. TG curves of compounds **1** and **2**.

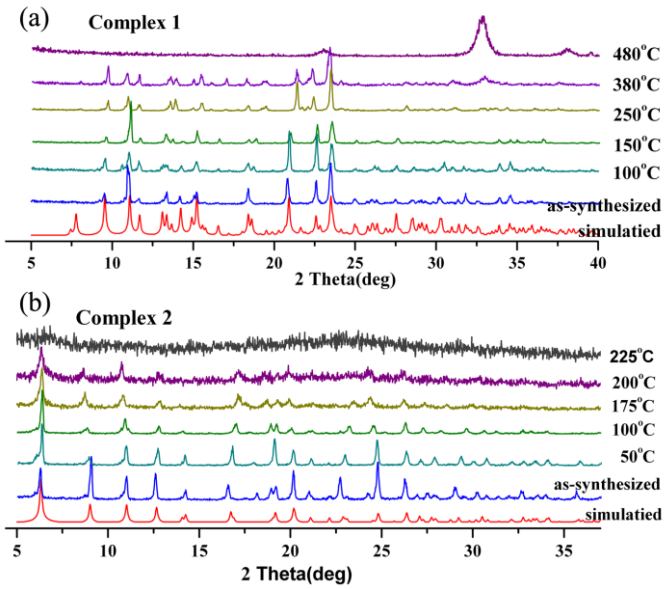

Figure S8. Temperature-variable XRPD patterns of **1** and **2**.